Clim Dyn (2013) 41:589–600
DOI 10.1007/s00382-012-1473-2

Projection of snow cover changes over China under RCP scenarios

Zhenming Ji · Shichang Kang

Received: 14 April 2012 / Accepted: 24 July 2012 / Published online: 5 August 2012

Abstract Snow cover changes in the middle (2040–2059) and end (2080–2099) of the twenty-first century over China were investigated with a regional climate model, nested within the global model BCC_CSM1.1. The simulations had been conducted for the period of 1950–2099 under the RCP4.5 and RCP8.5 scenarios. Results show that the model perform well in representing contemporary (1986–2005) spatial distributions of snow cover days (SCDs) and snow water equivalent (SWE). However, some differences between observation and simulation were detected. Under the RCP4.5 scenarios, SCDs are shortened by 10–20 and 20–40 days during the middle and end of the twenty-first century, respectively. Whereas simulated SWE is lowered by 0.1–10 mm in most areas over the Tibetan Plateau (TP). On the other hand, the spatial distributions of SWE are reversed between the middle and end terms in the northeast China. Furthermore, compared with the changes of RCP4.5 scenario, SCDs are reduced by 5–20 days in the middle period under RCP8.5 scenario with even larger decreasing amplitude in the end term. SWE was lowered by 0.1–2.5 mm in most areas except the northeast of China in middle term under RCP8.5 scenario. The great center of SCDs and SWE changes are always located over TP. The regional mean of SCDs and SWE for the TP and for China display a declining trend from 2006 to 2099 with more pronounced changes in the TP than in China as a whole. Under the RCP8.5 scenario, the changes are enhanced compared to those under RCP4.5.

Keywords Snow cover · Regional climate model · Projection · China

Z. Ji · S. Kang (✉)
Key Laboratory of Tibetan Environment Changes and Land Surface Processes, Institute of Tibetan Plateau Research, Chinese Academy of Sciences, 100101 Beijing, China
e-mail: shichang.kang@itpcas.ac.cn

Z. Ji
e-mail: jzm@itpcas.ac.cn

Z. Ji
Graduate University of Chinese Academy of Sciences, 100049 Beijing, China

S. Kang
State Key Laboratory of Cryospheric Science, Chinese Academy of Sciences, 730000 Lanzhou, China

1 Introduction

Snow cover affects the radiation balance of the earth-atmosphere system due to its high albedo characteristics. It is one of the important factors that cause atmospheric circulation anomalies (Gong et al. 2003; Fasullo 2004; Zhang et al. 2004; Dash et al. 2005). Meanwhile, processes of snow freezing and melting can also disturb the balance of material and energy which have significant impact on climate and environment (Qin 2002).

The response of snow cover variation is very sensitive to climate change. The occurrence of snowfall and melting were largely determined by temperature in the Northern Hemisphere (IPCC 2007). Due to the fast speed of global warming in the recent decades, decreasing trends of snow cover areas and depth occurred in some regions, such as western North America in spring (Groisman et al. 2004; Stewart et al. 2005; Mote 2006); central Europe (Scherrer et al. 2004; Vojtek et al. 2003; Falarz 2002) and so on. The temporal and spatial distributions of snow cover and their changes in China had been investigated based on observations, suggesting increased trends of snow depth and snow cover days in northwest China (Li 1999; Che 2006;

Qin et al. 2006) and Tibetan Plateau (Kang et al. 2010, You et al. 2011) in the last decades unalike the trends in North America and central Europe.

Projection of snow cover changes were generally implemented by global climate models (ACIA 2004; Sun et al. 2010). However, the coarse resolution of the global climate models had led to errors from simulated results, while high-resolution regional climate model could compensate for this deficiency (Gao et al. 2006; 2008). Shi et al. (2011) used a regional climate model with 25 km horizontal grid space to predict snow cover changes over China under A1B scenario (Nakicenovic et al. 2000).Yet, there are no results about the snow cover changes over China under representative concentration pathway (RCP) scenarios (Moss et al. 2008).

In this work, a regional climate model was used to simulate a period of 150 years over East Asia. Results showed that the model could well represent the basic climatology over this region (Ji 2012). In order to understand future changes of snow cover under RCP scenarios which might be contributing to the Intergovernmental Panel on Climate Change Fifth Assessment Report (IPCC AR5), changes in snow cover days (SCDs) and snow water equivalent (SWE) were investigated under RCP8.5 and RCP4.5 scenarios, respectively.

2 Model, data and experiments design

The Regional Climate Model version 4.0 (RegCM4) developed at Abdus Salam International Center for Theoretical Physics (ICTP) was used (Giorgi et al. 2012). RegCM4 is updated from the previous version of RegCM2 (Giorgi et al. 1993a, b) and RegCM3 (Pal et al. 2007). The series models of RegCM were widely applied in China, to address investigations on climate change (Gao et al. 2001, 2011, 2012), extreme events assessment (Gao et al. 2002), aerosols effects (Ji et al. 2010, 2011; Zhang et al. 2009), land use investigations (Gao et al. 2007; Zhang et al. 2010), and paleoclimate simulations (Ju et al. 2007).

We conducted a series of parametric sensitivity tests and finally set the model configuration to be as follows. Biosphere–Atmosphere Transfer Scheme (BATS1e) (Dickinson et al. 1993) was used to describe land surface processes. NCAR CCM3 radiation package was employed as the radiative transfer module. Convective precipitation was represented by the mass flux scheme of Grell (1993) with Arakawa and Schubert type closure (Arakawa and Schubert 1974), and the planetary boundary layer computation was assessed with the non-local formulation of Holtslag et al. (1990).

Initial and lateral boundary conditions were obtained from the global model outputs of the Beijing Climate Center-Climate System Model version 1.1 (BCC_CSM1.1) available on http://cmip-pcmdi.llnl.gov/cmip5/. BCC_CSM1.1 is composed by the following parts: the BCC_AGCM2.1 atmospheric model (Wu et al. 2010; Wu 2011), which is developed from NCAR CAM3.0 (Collins et al. 2004), the BCC_AVIM1.0 land surface model (Ji 1995; Dan et al. 2002), the ocean and sea-ice modules of MOM4-L40 (Griffies et al. 2004) and the SIS from Geophysical Fluid Dynamics Laboratory (GFDL). Horizontal resolution of BCC_AGCM2.1 is T42 ($\approx$280 km). The validation of the model performance shows good results about simulating the present climate (Wu et al. 2010; Zhang et al. 2011). BCC_CSM1.1 is one of the Chinese models participating the CMIP5 (Coupled Model Intercomparison Project Phase 5).

Two experiments were conducted from 1950 to 2099 (the first year is considered as model initialization/spin up time). We analyzed SCDs and SWE at present period from 1986 to 2005 (reference, RF), and in the future phase during 2006–2099 under RCP4.5 and RCP8.5 emission scenarios. RCP4.5 pathway is a stabilization of radiative forcing at 4.5 W/m^2 in 2100, while RCP8.5 simulates adapted emissions with stabilizing near 8.5 W/m^2. The period of 2040–2059 are considered as the middle of the twenty-first century (mid-term) and the period of 2080–2099 represents the end of the twenty-first century (end-term). The differences between RCP4.5 and RF (RCP4.5-RF) are considered as the changes of snow cover under the RCP4.5 scenario. Whereas RCP8.5 minus RCP4.5 (RCP8.5-RCP4.5) represents the changes under increasing emission concentration and it can also compare the changes between two different emission scenarios. In addition, the regional mean temporal evolution of annual mean SCDs and SWE changes of TP and China are discussed for the period between 2006 and 2099 (relative to 1986–2005).

The model horizontal resolution is 50 $\times$ 50 km, while the vertical configuration was set at 18 sigma layers with the model top at 10 hPa. Central point of the model was fixed at 35°N, 105°E, with 160 grids in the west-east direction and 109 grids for the north–south. Figure 1 shows the model domain and topography. The model domain covers the continent China and its neighboring countries. The locations of Tibetan Plateau, Xinjiang, Inner Mongolia, Northeast China and the other regions that we analyzed were marked on the map. RegCM4 describes well the topography, e.g. Tianshan Mountains, Qaidam Basin and Qilian Mountains in northwest China can be easily identified.

The daily datasets of snow depth were developed by Che et al. (2008) based on remote sensing data with the calibration from meteorological station observations. As did in Shi et al. (2011), a snow cover day is defined as a day when the snow depth is deeper than 1 cm in the observation data, and SWE must be greater than 1 mm in the simulation. SCDs is the total number of snow cover days during the

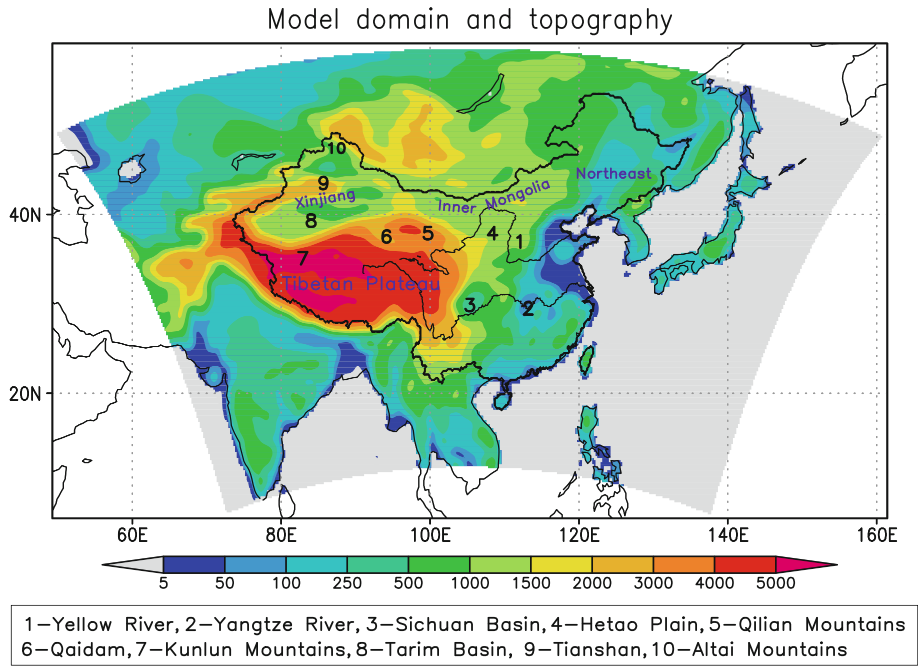

Fig. 1 Model domain and topography (units: meter)

annual snow cycle, which starts from the first day of September and ends on the last day of the following August.

Global Monthly EASE-Grid Snow Water Equivalent Climatology (Armstrong et al. 2007) datasets were used to compare with the simulated SWE. The observation dataset of CN05 (Xu et al. 2009) and Xie-Arkin (Xie et al. 2007) are used to validate the simulated surface air temperature and precipitation, respectively. These observations are given at the resolution of 0.5° × 0.5°.

3 Model performances

Previous studies have indicated that RegCM4 had a good performance for simulating the climate over China (Ji 2012). As shown in Fig. 2, simulated surface air temperature (Fig. 2b) follows generally that of the observations (Fig. 2a). It represents colder trends in the north and warming in the south over the flat areas of eastern China. While in western China, the distribution of temperature is largely affected by topography and shows significant temperature gradients. Compared with observations, the model captures the regional details well. For examples, the high values in the Tarim and Qaidam Basin, and low areas located in the Altai, Tianshan and Qilian Mountains are accurately represented by RegCM4.

In the mean time, the model reproduced the basic position of rain band over China. Annual mean precipitation shows a decrease from southeast to northwest (Fig. 2c), with greatest value exceeding 1500 mm in the southeastern coastal areas. In the northwest where arid and semi-arid climate prevails, the precipitation is less than 100 mm per year. Though the simulations (Fig. 2d) are not thoroughly representing the distribution of the observations, the precipitation patterns caused by topographical effects, e. g. the larger values in the Qilian Mountains and smaller values in the nearby Qaidam Basin, are captured well by RegCM4.

Figure 3 shows observed and simulated SCDs and SWE during RF period over China. TP, Northwest (except for the desert regions of Tarim Basin and Inner Mongolia) and Northeast China are the three great snow cover regions with annual mean SCDs usually exceeding 60 days (Fig. 3a). In the eastern plain areas along the north of the Yangtze River, the SCDs are in the range of 1–30 days, and there is almost no snow cover day in the Sichuan Basin, midwest Inner Mongolia and south of the Yangtze River. The simulated results (Fig. 3b) are basically consistent with the observations. Furthermore, the model captures the spatial characteristics in areas of complex terrain, such as the Tianshan Mountains, Qaidam Basin and Qilian Mountains in the northwest of China. Finally, the large overestimates of SCDs in the TP and Northeast China as simulated by RegCM3 (Shi et al. 2011) are improved in our experiments.

The model can also represent the spatial distribution of SWE (Fig. 3c, d). The pattern is similar with SCDs. In most areas of north Xinjiang, TP and northeast China, SWE are beyond 10 mm, while Tarim Basin, Midwest Inner Mongolia and southern China show values below 0.5 mm. Due to its higher resolution, the model simulates well also over high mountain regions (e. g. Tianshan, Altai Mountains and southeastern TP) where the values of SWE are greater than 75 mm.

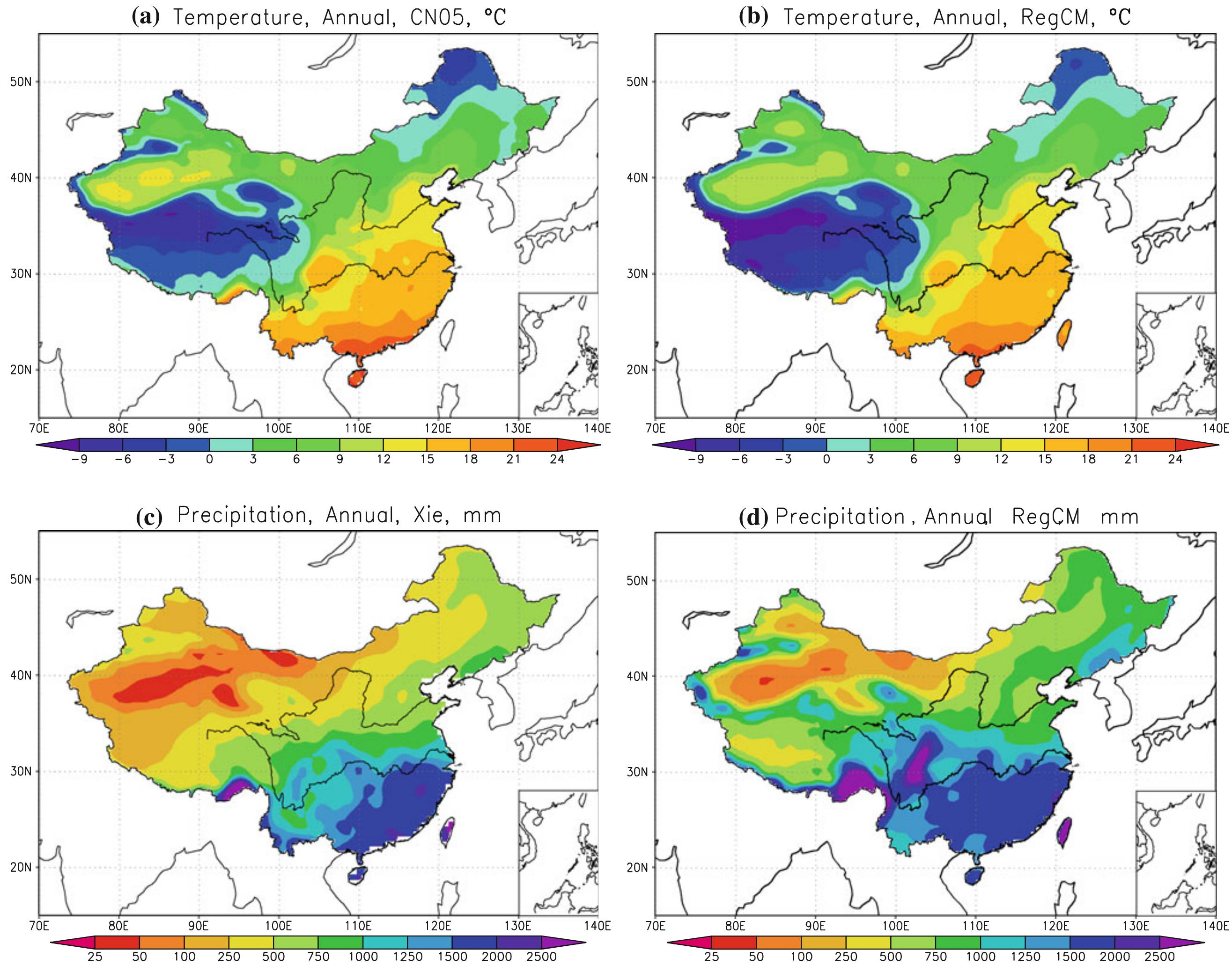

Fig. 2 Observed (**a**, **c**) and simulated (**b**, **d**) annual mean temperature (**a**, **b**) (units: °C) and precipitation (**c**, **d**) (units: mm) during 1986–2005

RegCM4 has a good simulation capability in the three major snow cover areas of China. However, some discrepancies can be found between observation and simulations. For instance, the model simulated SCDs are overestimated in the north of the TP, west of the Hetao Plain, and Tarim Basin. In particular, the greatest overestimate of SCDs appears in Kunlun Mountains located in northern TP. The snowfall processes are determined both by air temperature (less than 0 °C) and precipitation in the model, while the cold and wet bias often occurs in high altitude regions (Shi 2010; Gao et al. 2011) leading to greater snowfall and delayed snowmelt.

4 Projection of snow cover changes

4.1 Changes of SCDs

The differences in spatial distribution of annual mean SCDs changes (RCP4.5-RF, RCP8.5-RCP4.5) of are shown in Fig. 4. Annual mean SCDs decline over the main snow cover areas during the mid-term in the RCP4.5 scenario compared to RF simulation (Fig. 4a). In northern Xinjiang, Inner Mongolia, eastern TP and northeast China, SCDs decrease by 10–20 days, while the other regions show relatively small changes. At the end-term (Fig. 4b), the spatial distribution of SCDs changes is similar to that during the mid-term's. And the depleted areas are extended in the east and in the north of Sichuan Basin. Meanwhile, the decreased intensity is greater than that in the mid-term and values are ranging between −20 and −30 days. In the Three-River-Source areas (the place where Yangtse, Yellow and Lantsang River originate in the central TP) and in parts of the southern TP, SCDs are reduced by more than 30 days.

SCDs decrease in the TP and central China during the mid-term in the RCP8.5 scenario compared with RCP4.5's results (Fig. 4c). Spatial decreasing is obvious over the TP with values of −5 to −20 days. At the end-term (Fig. 4d), the amplitude of changes has been more enhanced in the

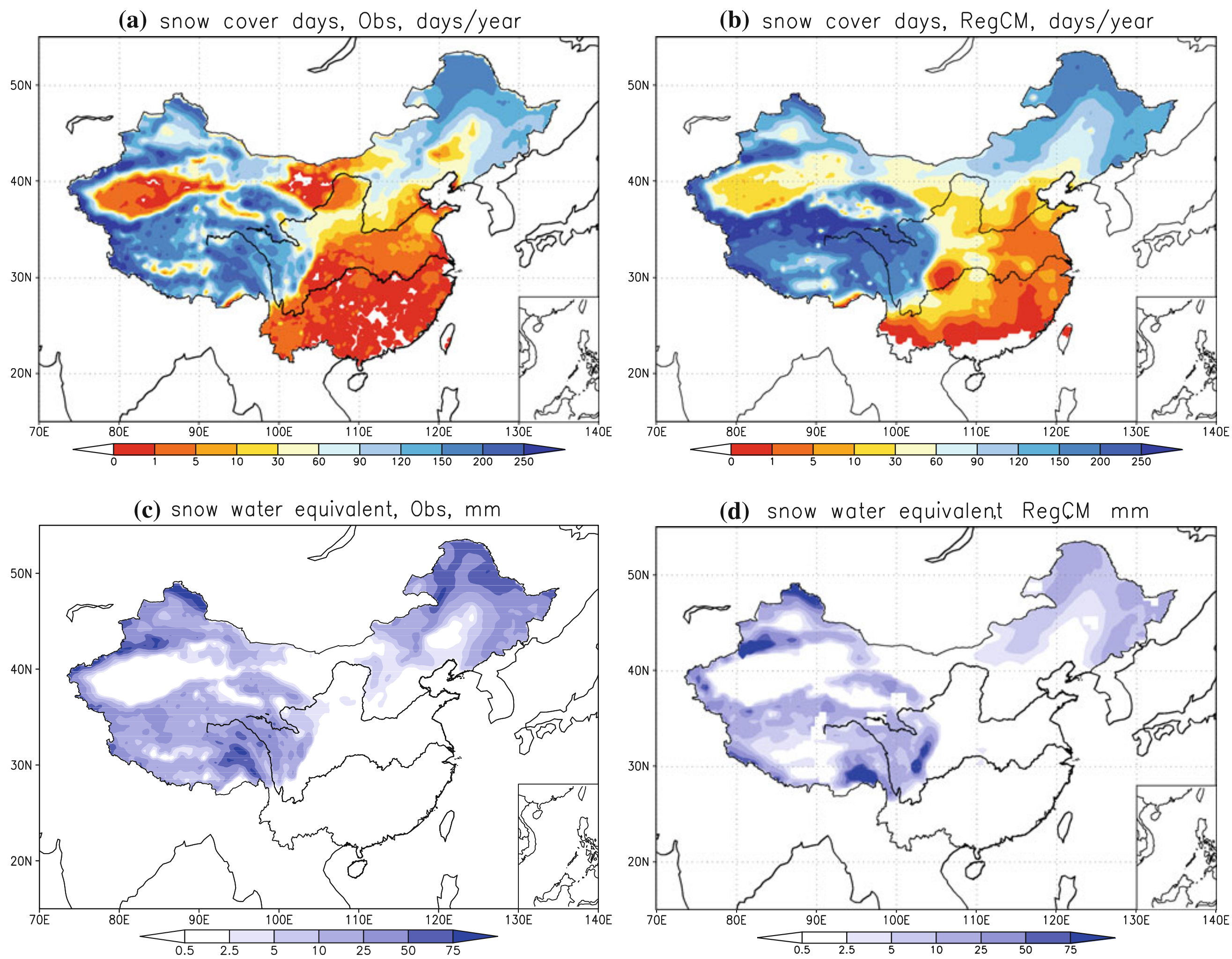

Fig. 3 Observed (**a**, **c**) and simulated (**b**, **d**) annual mean SCDs (**a**, **b**) (units: days/year) and SWE (**c**, **d**) (units: mm) during 1986–2005

three snow cover areas compared to the mid-term's. SCDs will reduce significantly, reaching over 20 days of difference with the largest center located in the TP.

SCDs are shortened over China in future under the RCP4.5 scenario. Decreased intensity at the end-term is greater than the results of mid-term in the TP. While the concentration of greenhouse gas emission is increased, larger reduction of SCDs occurs in the TP than that in the other parts of China. Changes of temperature greatly impact the variations of snow cover. Figure 5 shows temperature increases in two terms under the RCP4.5 and RCP8.5 scenarios, respectively. In general, warming in north China and TP is greater than those in the other regions. The increased amplitude in the end-term (Fig. 5c, d) is larger than that in the mid-term's (Fig. 5a, b). Temperature increases can affect snowfall and snowmelt. Compared with Figs. 4 and 5, the distributions are significantly more similar in the corresponding regions. For example, the differences of temperature between RCP8.5 and RCP4.5 in the mid-term (Fig. 4c) shows warming almost over the whole TP, while smaller changes are shown in the other areas of China. It is noteworthy that SCDs are mainly decreased in the plateau and changes in the other regions are not apparent in the same period. Though precipitation increases in two terms in the north China (Fig. 6), the distributions of precipitation changes do not match with those of SCDs'.

Due to the large snow-covered areas, the influence of temperature on SCDs in the TP are much greater than in the other regions of China's under the background of global warming. Thus, in the future, the sensitivities between SCDs and temperature seem to increase in the TP. This conclusion is consistent with the prognosis of Ma et al. (2010) which were based on the observed data.

4.2 Changes of SWE

Spatial changes of SWE are different from those of SCDs'. Figure 7a depicts the changes of SWE over China under

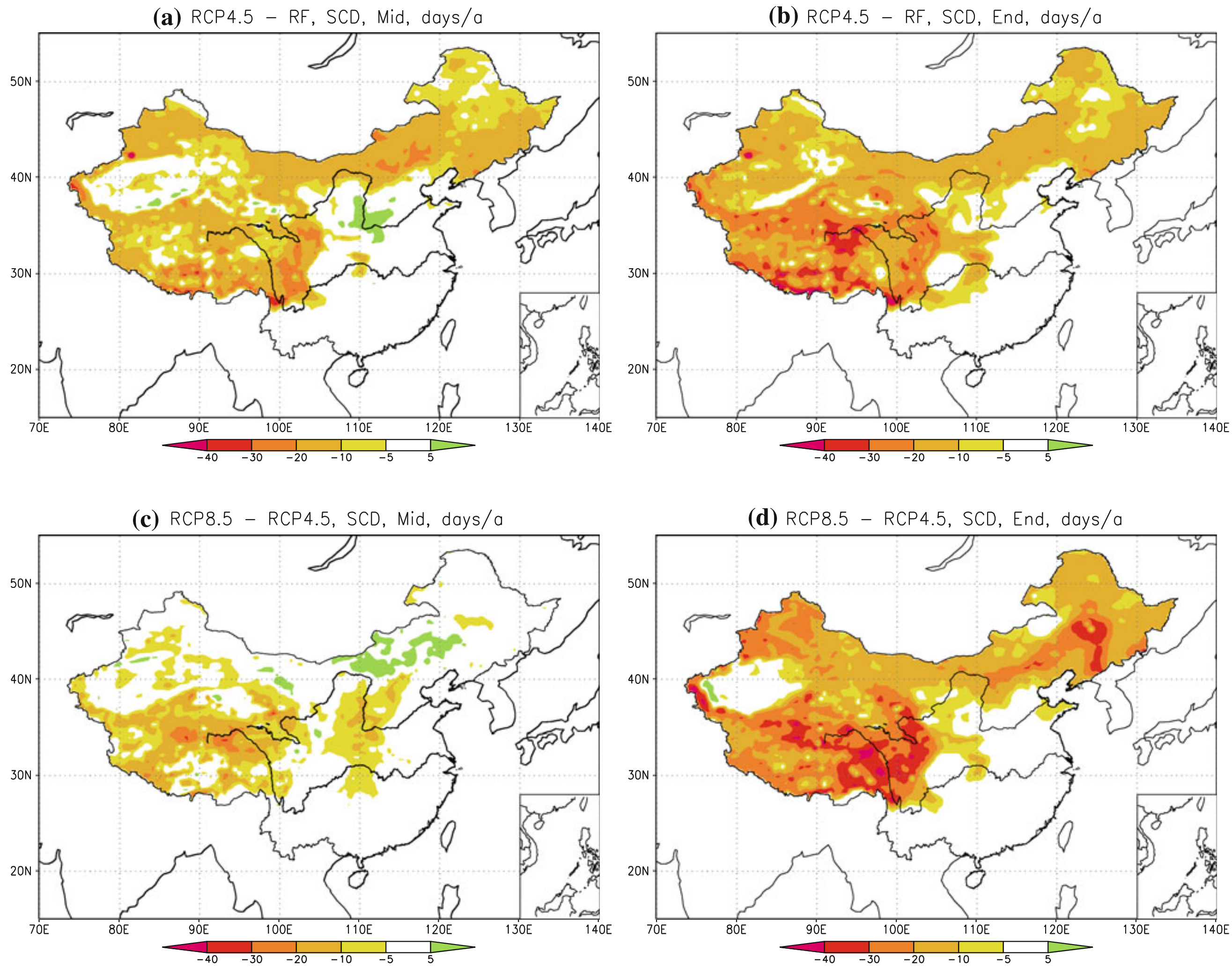

Fig. 4 Differences in annual mean SCDs changes in the mid-term and the end-term (units: days/year) (**a** RCP4.5-RF in the mid-term; **b** RCP4.5-RF in the end-term; **c** RCP8.5-RCP4.5 in the mid-term; **d** RCP8.5-RCP4.5 in the end-term)

RCP4.5 scenario in the mid-term. In eastern and southern TP, northern Xinjiang and central of northeast China, SWE show a reduction of −1 to −10 mm. However, regions with SWE values ranging between 0.1 and 2.5 mm are to be found in the north of northeast and central China. At the end-term, the spatial distribution of SWE in the TP and Northwest China are consistent with the mid-term's pattern (Fig. 7b). Although, changes of SWE are different from the former results in central China where there are decrease or less changes are found. The areas with increased SWE in the north of northeastern China show an expansion and the largest center is beyond 2.5 mm. It is noted that the SCDs are shortened in northeastern China, while the SWE is increased. That may be due to the fact that the extreme snowfall events might strengthen (Sun et al. 2010).

The difference of SCD between RCP8.5 and RCP4.5 (RCP8.5–RCP4.5) scenarios in the mid-term show significant decrease of SWE are clearly in the north of TP (Fig. 7c). It decreases by 0.1–1 mm in the central and eastern China, while increases in most parts of northeastern China can be found. At the end-term (Fig. 7d), SWE reduces more than 10 mm in the TP and in the northwest of China. Contrary to the increase of SWE in northeastern China, a reduction of 5 mm is simulated.

SCDs and SWE show a general consistent decrease in north of TP and Xinjiang during the two terms of the twenty-first century, while a reversed situation appears in the northeast of China under the RCP4.5 scenario. The simulated results of SCDs show similar distribution with Shi et al. (2011), which estimated the snow cover changes by using RegCM3 under the IPCC A1B scenario suggesting that the changes of values were between RCP4.5's and RCP8.5's. However, changes in SWE are partly different from the former research which displayed on the positive distribution (Shi et al. 2011). The reduction of SWE is also significantly greater than the results of RCPs scenarios for the same

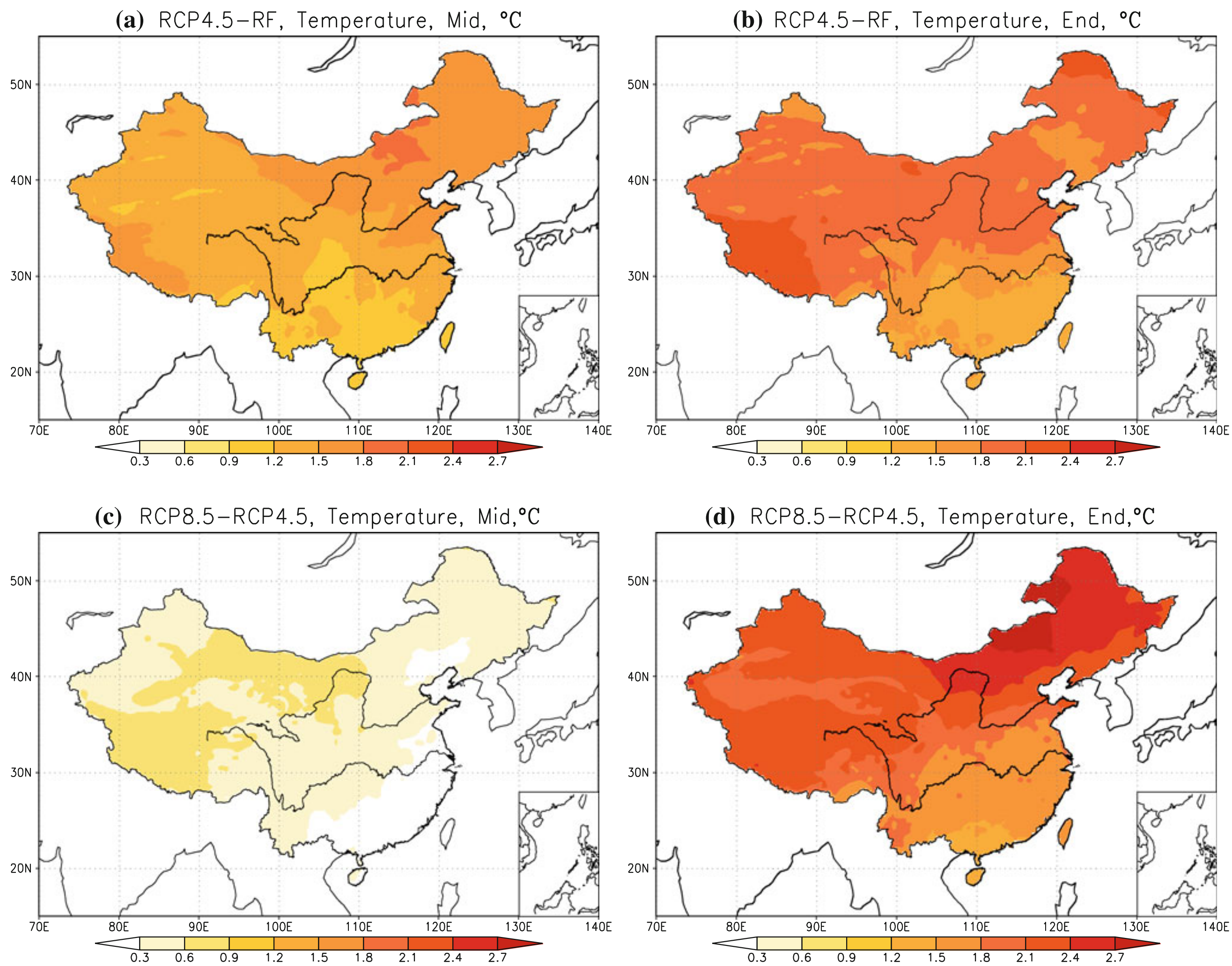

Fig. 5 Differences in annual mean temperature changes in the mid-term and the end-term (units: °C) (**a** RCP4.5-RF in the mid-term; **b** RCP4.5-RF in the end-term; **c** RCP8.5-RCP4.5 in the mid-term; **d** RCP8.5-RCP4.5 in the end-term)

period. For example, reduced values exceed 10 mm in the TP under A1B scenario, while they are reported less than 10 mm under the two RCP scenarios. The same tendency is also represented from multi-GCM (global climate model) ensemble outputs of CMIP3 (Coupled Model Intercomparison Project Phase 3) (e.g. Ma et al. 2011; Wang et al., 2010), while the magnitude of SWE changes are still different. It is noted that the uncertainties are prevalent in the projection of SWE under different scenarios.

4.3 Changes in the regional mean

Figure 8 shows the regional mean changes of the annual cycle of SCDs. Decreases of SCDs can be found in all the months, both at mid- and end-term, and under the two scenarios. Magnitudes of the decrease under RCP8.5 at the end-term are clearly larger than those of RCP4.5 at the mid-term, RCP4.5 at the end-term and RCP8.5 at the mid-term, all of which show similar patterns. The greatest reduction appears in autumn (September–November) with the maximum in November, followed by winter (December–February) and spring (March–May). The least changes occur in summer (June–August) when snowfall events are rare. In general, snowfall over China starts in autumn and ends in early summer in the following year. It is noted that the reduced SCDs in autumn and spring are supported by the prediction that the snow cover starting date advances while the ending date delays in future (Shi et al. 2011).

Changes of regional mean of SCDs and SWE in the TP and the whole of China (CN) from 2006 to 2099 suggest decreased SCDs in CN and TP from 2006 to 2099 (Fig. 9). The linear trend of the TP is greater than that of CN. Changes of SCDs are ranged from −10 to 0 days in CN and −30 to 0 days in the TP (Fig. 9a). Under the RCP8.5 scenario (Fig. 9b), the linear trends are also declining in both CN (2 days/decade) and TP (3.7 days/decade). However,

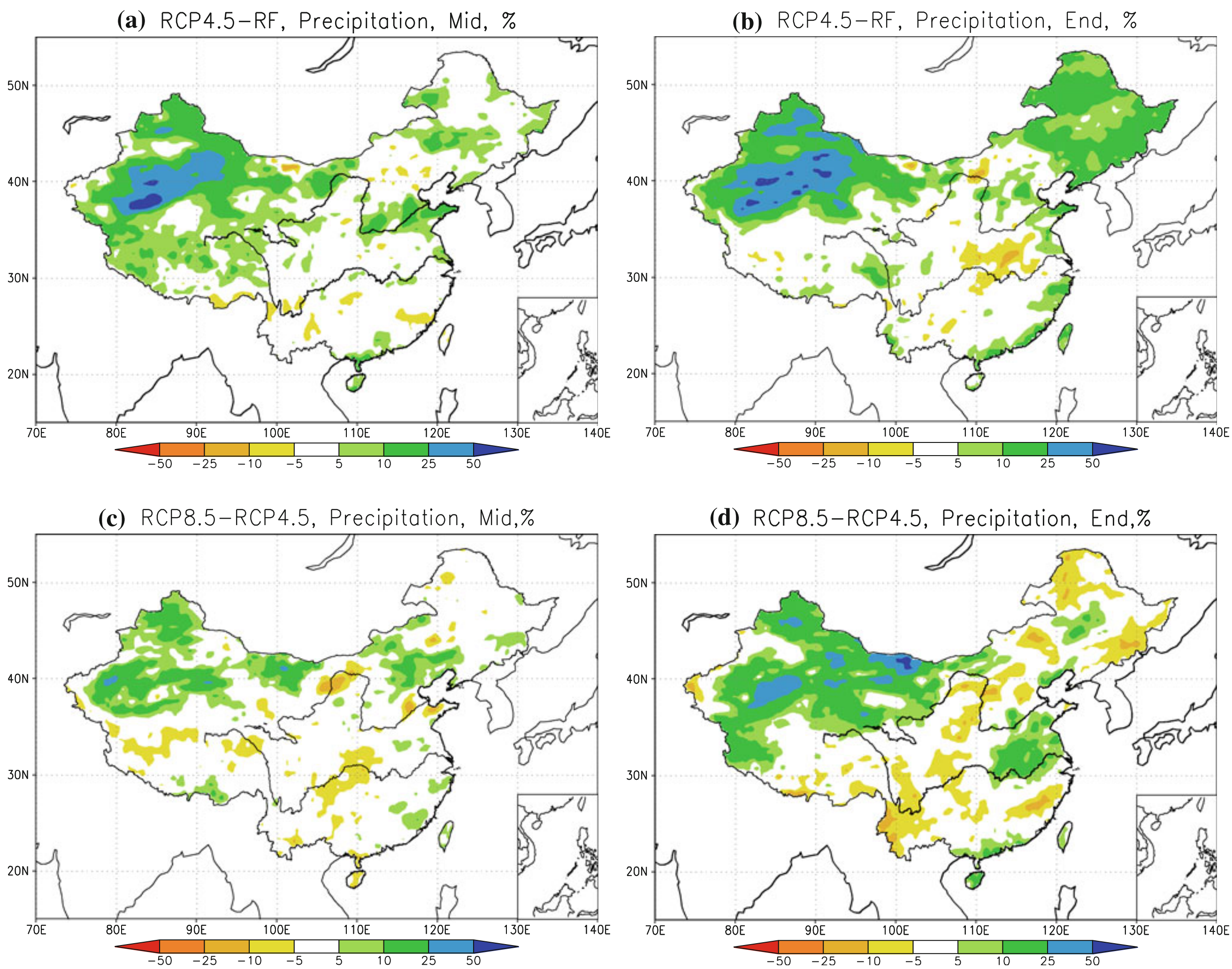

Fig. 6 Differences in annual mean precipitation changes in the mid-term and the end-term (units: %) (**a** RCP4.5-RF in the mid-term; **b** RCP4.5-RF in the end-term; **c** RCP8.5-RCP4.5 in the mid-term; **d** RCP8.5-RCP4.5 in the end-term)

the amplitude is enlarged in the TP. The range of SCDs' in CN was −20 to 0 days and −50 to 0 days in the TP.

Trends of SWE (Fig. 9c) are also reduced under both scenarios. The value ranges are −3 to 1 mm in CN and −4 to 1.5 mm in the TP. Clearly the trend of declining in TP is larger than that in CN. More dramatic decreasing is suggested under the RCP8.5 scenario (Fig. 9d) than those under the RCP4.5 scenario. The outline patterns of TP and CN are similar with those under the A1B scenario, while the decreased intensities of SWE are quite different. For instance, the linear trends of TP are 1.5 mm/decade under A1B's (Shi et al. 2011), however, they are just 0.3 and 0.5 mm/decade under RCP4.5's and RCP8.5's, respectively.

5 Summaries

A regional climate model was used to conduct two experiments under RCPs scenarios to investigate the snow cover changes in the twenty-first century. The capability of model was evaluated by comparing the simulations against observations firstly followed by the analysis of SCDs and SWE changes under RCP4.5 and RCP8.5 scenarios.

The results show that model can reproduce the spatial distribution of SCDs and SWE over China. The main discrepancies of the model simulation are the overestimation of SCDs and SWE compared with the observations. The errors in climatology over west China from model simulation are the primary reason for generating the bias between simulated and observed SWE.

SCDs decrease both at the middle and at the end of twenty-first century under RCP4.5 scenario. SWE is mostly reduced except in parts of northeast and central China. Under RCP8.5 scenario, the amplitude of reduced SCDs and SWE are greater than their changes under RCP4.5 scenario. The larger center is always found to be located in the TP. That is due to increased greenhouse gasses that changed the temperature over China and exhibit impacts on

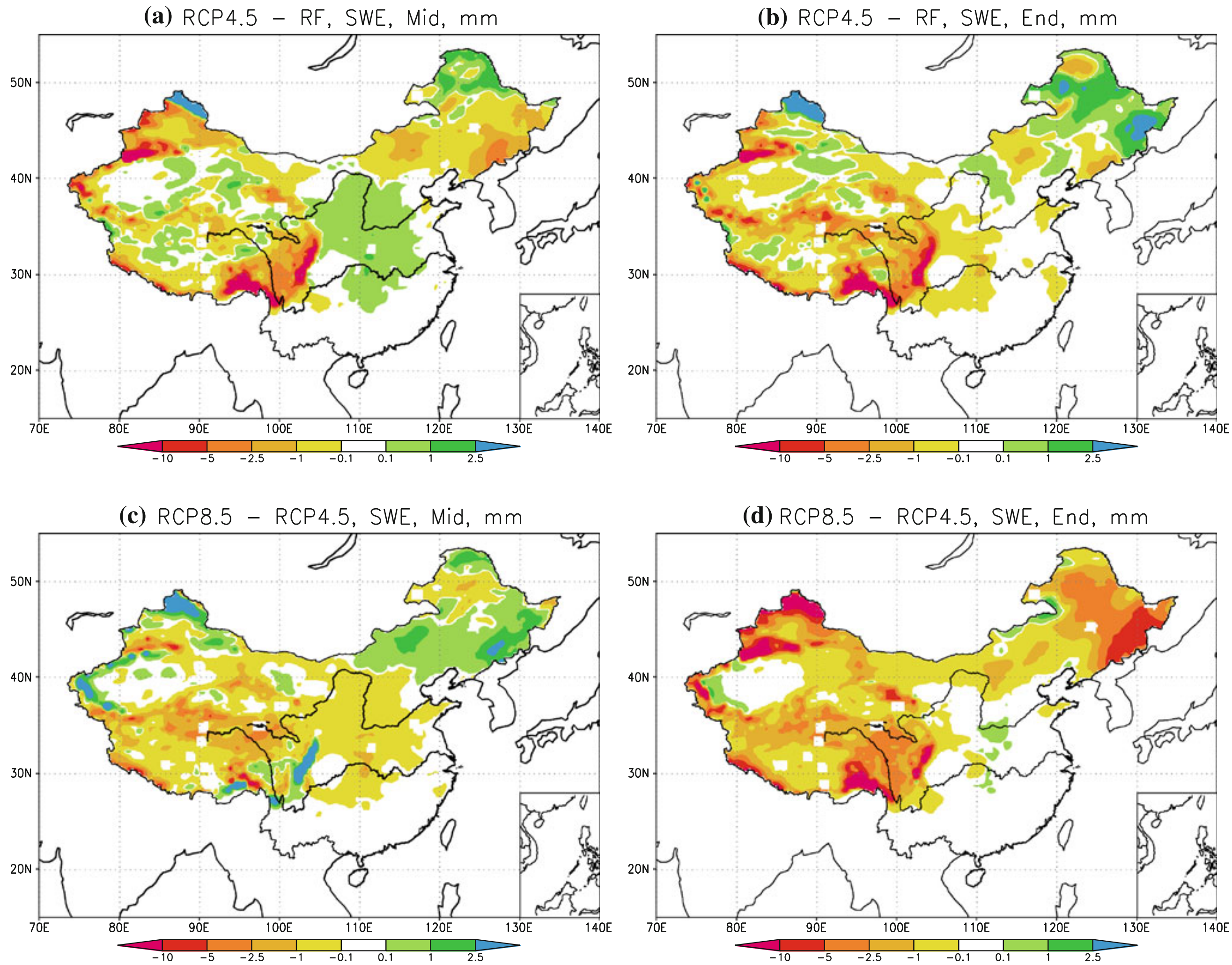

Fig. 7 Differences in annual mean SWE changes in the mid-term and the end-term (units: mm) (**a** RCP4.5-RF in the mid-term; **b** RCP4.5-RF in the end-term; **c** RCP8.5-RCP4.5 in the mid-term; **d** RCP8.5-RCP4.5 in the end-term)

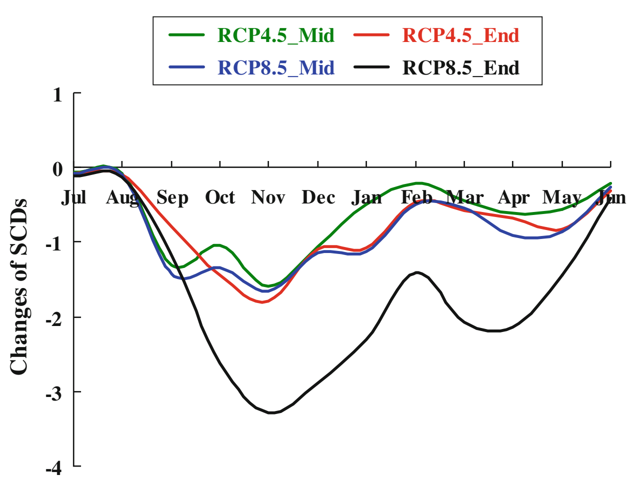

Fig. 8 Annual cycle of SCDs changes in the mid-term and the end-term under RCP4.5 and RCP8.5 scenarios, respectively (units: days/year)

snow cover. However, snow cover in the plateau shows greatest sensitivity to climate change. The regional mean SCDs and SWE of TP and China show declining trend from 2006 to 2099. The fluctuant reduction of TP is significantly greater than the national average. While the concentration of greenhouse gas emissions increased, the respective changes get enhanced. It is implied that emission reductions could decelerate snow cover changes in the future.

Still large uncertainties exist in the projection of snow cover changes in the present days. Of them, precipitation as is one of the main factors affecting snow cover changes, show larger uncertainties and differences among different models and emission scenarios. The CORDEX (COordinated Regional climate Downscaling EXperiment) international program has been proposed (Giorgi et al. 2009), try to carried out dynamic downscaling of utilizing regional climate model simulations driven by multiple GCM

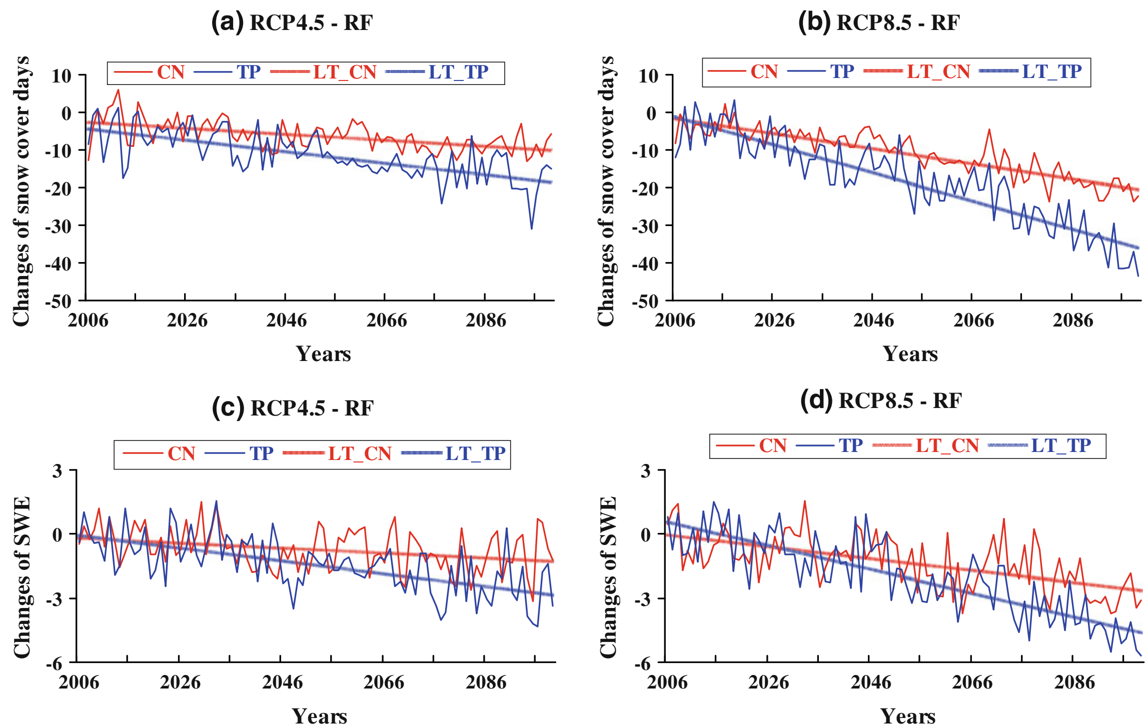

Fig. 9 Changes of regional mean SCDs (**a**, **b**) and SWE (**c**, **d**) in the TP and CN during 2006–2099 (LT means liner trend) (units: SCDs: days/year; SWE: mm)

outputs (e. g. CMIP5 results) at different regions of the world (Giorgi et al. 2012; Sylla et al. 2010; Wu 2012). The outcomes of CORDEX can contribute in exploring and reducing the uncertainties.

Our future research will be not only limited to snow cover and its impact on the climate and environment, but will combine with the effects and detection of aerosols deposited on snow in ITPCAS (Institute of Tibetan Plateau Research, Chinese Academy of Sciences) (Xu et al. 2009). A snow—black soot feedback module will be coupled with RegCM4 in the future, which will indeed help in the study of the impacts and feedbacks of aerosols deposition in the Tibetan Plateau.

Acknowledgments This study was supported by the Globe Change Research Program of China (2010CB951401) and National Nature Science Foundation of China (41190081, 40830743). We thank Dr. Xiaoge Xin for providing the outputs of BCC_CSM1.1, and Ms. Zoe Lucia Lüthi for suggestions of the written English.

References

ACIA (2004) Arctic climate impact assessment (ACIA): impact of a warming arctic. Cambridge University of Press, New York

Arakawa A, Schubert WH (1974) Interaction of a cumulus cloud ensemble with the large-scale environment, Part I. J Atmos Sci 31(3):674–701

Armstrong RL et al (2007) Global Monthly EASE-Grid Snow Water Equivalent Climatology. National Snow and Ice Data Center. Digital media, Boulder, CO

Che T (2006) Study on passive microwave remote sensing of snow and snow data assimilation method. Doctoral dissertation, Cold and Arid Regions Environmental and Engineering Research Institute, Chinese Academy of Sciences, Lanzhou, 105 pp. (In Chinese)

Che T et al (2008) Snow depth derived from passive microwave remote-sensing data in China. Ann Glaciol 49 (1):145–154 (10)

Collins WD et al (2004) Description of the NCAR community atmosphere model (CAM3). Technical report NCAR/TN-464 + STR, National Center for Atmospheric Research, Boulder, Colorado, 226 pp

Dan L et al (2002) Climate simulations based on a different-grid nested and coupled model. Adv Atmos Sci 19(3):487–499

Dash SK et al (2005) Response of the Indian summer monsoon circulation and rainfall to seasonal snow depth anomaly over Eurasia. Clim Dyn 24:1–10

Dickinson RE et al (1993) Biosphere-atmosphere transfer scheme (BATS) version1e as coupled to the NCAR community climate model. NCAR Tech. Note NCAR/TN-387 + STR, National Center for Atmospheric Research

Falarz M (2002) Long-term variability in reconstructed and observed snow cover over the last 100 winter seasons in Cracow and Zakopane (South Poland). Clim Res 19(3):247–256

Fasullo J (2004) A stratified diagnosis of the Indian Monsoon-Eurasian snow cover relationship. J Clim 17:1110–1122

Gao XJ et al (2001) Climate change due to greenhouse effects in China as simulated by a regional climate model. Adv Atmos Sci 18(6):1224–1230

Gao XJ et al (2002) Changes of extreme events in regional climate simulations over East Asia. Adv Atmos Sci 19(5):927–942

Gao XJ et al (2006) Projected changes in mean and extreme precipitation over the Mediterranean region from a high resolution double nested RCM simulation. Geophys Res Lett 33:L03706. doi:10.1029/2005GL024954

Gao XJ et al (2007) Simulation of land use effects on climate in China by RegCM3. Sci China Ser D-Earth Sci 50:620–628

Gao XJ et al (2008) Reduction of future monsoon precipitation over China: comparison between a high resolution RCM simulation and the driving GCM. Meteor Atmos Phys 100:73–86

Gao XJ et al (2011) A high resolution simulation of climate change over China. Sci China Earth Sci 54:462–472

Gao XJ et al (2012) Uncertainties in monsoon precipitation projections over China: results from two high-resolution RCM simulations. Climate Res 52:213–226

Giorgi F et al (1993a) Development of a second-generation regional climate model (RegCM2). Part I: boundary-layer and radiative transfer processes. Mon Weather Rev 121:2794–2813

Giorgi F et al (1993b) Development of a second-generation regional climate model (RegCM2). Part II: convective processes and assimilation of lateral boundary conditions. Mon Weather Rev 121:2814–2832

Giorgi F et al (2009) Addressing climate information needs at the regional level. The CORDEX framework. WMO Bull 58(3): 175–183

Giorgi F et al (2012) RegCM4: model description and preliminary tests over multiple CORDEX domains. Clim Res 52:7–29

Gong G et al (2003) Relative impacts of Siberian and North American snow anomalies on the winter Arctic Oscillation. Geophys Res Lett 30(16):1848. doi:10.1029/2003GL017749

Grell GA (1993) Prognostic evaluation of assumptions used by cumulus parameterizations. Mon Weather Rev 121:764–787

Griffies SM et al (2004) A technical guide to MOM4. GFDL Ocean group technical report no. 5. NOAA/Geophysical Fluid Dynamics Laboratory, 371 pp

Groisman PY et al (2004) Contemporary changes of the hydrological cycle over the contiguous United States: Trends derived from the situ observations. J Hydrometeorol 5:64–85

Holtslag AAM et al (1990) A high resolution air mass transformation model for short-range weather forecasting. Mon Weather Rev 118:1561–1575

IPCC (2007) Summary for policymaker of climate change 2007: the physical science basis. Contribution of working group I to the fourth assessment report of intergovernmental panel on climate change. Cambridge University Press, Cambridge

Ji JJ (1995) A climate-vegetation interaction model: simulating physical and biological processes at the surface. J Biogeogr. doi:10.2307/2845941

Ji ZM (2012) Simulation of the climate change over China under RCPs scenarios by a high resolution regional climate model. Doctoral dissertation, Institute of Tibetan Plateau Research, Chinese Academy of Sciences, Beijing, 137 pp (In Chinese)

Ji ZM et al (2010) Simulation of the aerosols over Asia and its climate effect on China. Chin J Atmos Sci 34(2):262–274 (In Chinese)

Ji ZM et al (2011) Simulation of anthropogenic aerosols over South Asia and their effects on Indian summer monsoon. Clim Dyn 36:1633–1647

Ju LX et al (2007) Simulation of the Last Glacial Maximum climate over East Asia with a regional climate model nested in a general circulation model. Palaeogeogr Palaeoclimatol Palaeoecol 248:376–390

Kang SC et al (2010) Review of climate and cryospheric change in the Tibetan Plateau. Environ Res Lett. doi:10.1088/1748-9326/5/1/015101

Li PJ (1999) Variation of snow water resources in northwestern China, 1951–1997. Sci China Ser D-Earth Sci 42 (S1), 72-79 (In Chinese)

Ma LJ et al (2010) Analysis of air temperature sensitivity of snow cover days on the Qinghai-Tibetan Plateau. Adv Clim Change Res 6(1):1–7

Ma LJ et al (2011) Snow water equivalent over Eurasia in next 50 years projected by CMIP3 models. J Glaciol Geocryol 33(4):707–720 In Chinese

Moss R et al (2008) Towards new scenarios for analysis of emissions, climate change, impacts, and response strategies. Intergovernmental Panel on Climate Change, Geneva

Mote PW (2006) Climate-driven variability and trends in mountain snowpack in west North American. J Clim 19(23):6209–6220

Nakicenovic N et al (2000) Special report on emissions scenarios: a special report of working group III of the intergovernmental panel on climate change. Cambridge University Press, Cambridge, UK

Pal JS et al (2007) Regional climate modeling for the developing world: the ICTP RegCM3 and RegCNET. Bull Am Meteorol Soc 88(9):1395–1409

Qin DH (ed) (2002) Assessment on the environment change of West China. Science Press, Beijing In Chinese

Qin DH et al (2006) Snow cover distribution, variability, and response to climate change in western China. J Clim 19(9):1820–1833

Scherrer SC et al (2004) Trends in Swiss alpine snow days—the role of local and large scale climate variability. Geophys Res Lett 31:L13215. doi:10.1029/2004GL020255

Shi Y (2010) A high resolution climate change simulation of the 21st century over East Asia by RegCM3. Doctoral dissertation, Institute of Atmospheric Physics, Chinese Academy of Sciences, Beijing, 118 pp (In Chinese)

Shi Y et al (2011) Changes in snow cover China in the 21st century as simulated by a high resolution regional climate model. Environ Res Lett. doi:10.1088/1748-9326/6/4/045401

Stewart IT et al (2005) Changes towards earlier streamflow timing across western North American. J Clim 18:1136–1155

Sun JQ et al (2010) Spatial–temporal features of intense snowfall events in China and their possible change. J Geophys Res 115:D16110

Sylla MB et al (2010) Multiyear simulation of the African climate using a regional climate model (RegCM3) with the high resolution ERA-interim reanalysis. Clim Dyn 35:231–247

Vojtek M et al (2003) Some selected snow climate trends in Slovakia with respect to altitude. Acta Meteorologica Universitatis Comenianae 32:17–27

Wang CH et al (2010) A prediction of snow cover depth in the northern Xinjiang in the next 50 years. J Glaciol Geocryol 32(6):1059–1065 (In Chinese)

Wu TW (2011) A mass-flux cumulus parameterization scheme for large-scale models: description and test with observations. Clim Dyn. doi:10.1007/s00382-011-0995-3

Wu J (2012) Regional climate change simulations and uncertainty analysis over CORDEX-East Asia region. Doctoral dissertation, Chinese Academy of Meteorology Sciences, Beijing, 124 pp (In Chinese)

Wu TW et al (2010) The Beijing Climate Center atmospheric general circulation model: description and its performance for the present-day climate. Clim Dyn 34(1):123–147

Xie PP et al (2007) A gauge-based analysis of daily precipitation over East Asia. J Hydrol 8(3):607–626

Xu BQ et al (2009) Black soot and the survival of Tibetan glaciers. Proc Nat Acad Sci USA 106(52):2114–2118

You QL et al (2011) Changes of snow depth and snow day in the eastern and central Tibetan Plateau from observational data. Clim Res 46:171–183. doi:10.3354/cr00985

Zhang YS et al (2004) Decadal change of the spring snow depth over the Tibetan Plateau: the associated circulation and influence on the East Asian summer monsoon. J Clim 17:2780–2793

Zhang DF et al (2009) Simulation of dust aerosol and its regional feedbacks over East Asia using a regional climate model. Atmos Chem Phys 9:1095–1110

Zhang DF et al (2010) Agriculture-derived land use effects on climate over China as simulated by a regional climate model. ACTA Meteorologica Sinica 24(2):215–224

Zhang L et al (2011) Changes in precipitation extremes over Eastern China simulated by the Beijing Climate Center Climate System Model (BCC_CSM1.0). Clim Res 50:227–245